

## INVESTIGATION OF ELECTRON BUNCHES IN A MICROTRON

V. P. BYKOV

Physics Laboratory, Academy of Sciences U.S.S.R.

Submitted to JETP editor January 25, 1961

J. Exptl. Theoret. Phys. (U.S.S.R.) 40, 1658-1666 (June, 1961)

A technique is developed for measuring charge density in electron bunches produced when electrons are accelerated in a microtron. Measurements performed on the microtron of the Institute for Physics Problems showed that the effective length of the bunches is  $0.05 - 0.07\lambda$ , where  $\lambda$  is the wavelength of the accelerating field. The electron distribution in a bunch corresponds on the whole to the theory of microtron operation.

THE principle of the microtron, which is a powerful source of bunched electrons, was published as long ago as 1944.<sup>1</sup> The earliest microtrons<sup>2,3</sup> had low efficiency, owing to the difficulty of capturing electrons into accelerating orbits. The electrons were obtained through unregulated cold emission and were captured in a region traversed by all orbits. These difficulties were overcome and the current considerably increased in the microtron of the Institute for Physics Problems (IPP).<sup>4</sup>

A limit to the increase of current and energy in a microtron is imposed by the requirement of coherent emission of electron bunches. It is therefore of interest to investigate the size of bunches experimentally.

Electron bunching in microtrons depends mainly on the size of the region of phase stability, which was investigated theoretically by Henderson et al.<sup>5</sup> and by Kolomenskii.<sup>6</sup> The former gave numerical results, while the latter used an analytic method supplemented by numerical calculations. The results of the two investigations are in essential agreement.

From Kolomenskii's work it follows that stable phases range from 0 to  $32.5^\circ$ , in accordance with the inequality\*

$$0 < \text{tg}\varphi_s < \text{tg}(\varphi_s)_{\text{lim}} = 2/\pi.$$

A particle traversing the resonator will undergo phase oscillations if it is not in a stable phase. The frequency  $\nu$  of these oscillations at small amplitudes is given by

$$\cos\nu = 1 - \pi \text{tg}\varphi_s.$$

The departure of  $\nu$  from this equation increases with the amplitude of phase oscillations (see Fig. 4 in reference 6). Phase trajectories can be

\*tg = tan.

plotted in a plane, with ordinates representing the difference between the particle energy and the corresponding stable energy, and with abscissas representing the phase. The phase trajectories remain closed up to a certain limiting amplitude. The limiting trajectory bounds the phase stability region of the microtron. The longitudinal dimension of bunches in a microtron beam is obviously determined mainly by the extent of the phase stability region along the abscissal axis. Theoretical calculations show that the length of bunches must be about  $0.1\lambda$ , where  $\lambda$  is the wavelength of the accelerating field.

An oscilloscopic study of electron bunching was made on the IPP microtron operated in its first mode<sup>4</sup> and producing a 5 milliamp pulsed current at 7.3 Mev in the 12th orbit. This method had been used previously by Tzopp<sup>7</sup> to investigate electron bunching in a linear accelerator. The sweep was produced by a sinusoidal voltage of the same frequency as the accelerating frequency. All electron bunches traversed the deflecting system in the same phase, but the beginning and end of each bunch were in slightly different phases and were deflected differently. The bunch size was determined from these deflections and the sweep speed.

The deflecting system was a toroidal resonant cavity, where the electric field was perpendicular to the electron velocity. This resonator was placed in the 12th (i.e., last) orbit of the microtron (Fig. 1). Electrons were deflected vertically, i.e., parallel to the magnetic field of the microtron. Power was fed to the resonator from the waveguide of the microtron by means of a coaxial line.

A fluorescent screen was positioned 360 mm after the resonator along the 12th orbit. An electron bunch traced a bright vertical band on this screen, which was observed visually by television.

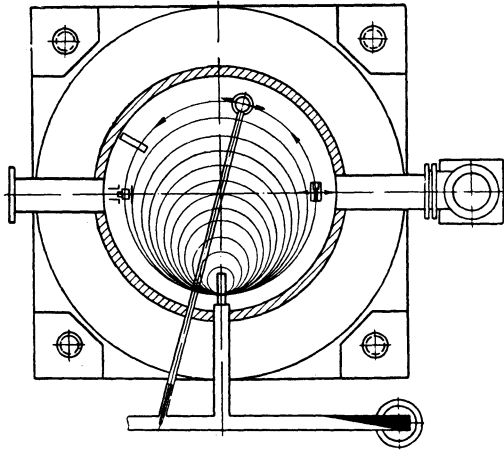


FIG. 1. General scheme of microtron.

The height  $h$  of this band was related to the bunch length  $l$  by

$$h/u = l/v, \quad (2)$$

where  $u$  is the sweep rate and  $v$  is the electron velocity ( $v \approx c$ ). Thus

$$l \approx hc/u. \quad (3)$$

For the purpose of determining the sweep rate, the deflection amplitude  $A$  must be known, i.e., the maximum deflection for the given resonator power, since  $u = \omega A$ . However, zero deflection accompanied the maximum sweep rate. Therefore the phase difference between the rf oscillations in the sweep resonator and the electron bunches had to be changed by at least  $\pi/2$ .

Since it was difficult to construct a phase shifter that would not affect the power in the sweep resonator, we employed a different measuring technique free of this defect. The sweep resonator was now shifted along the electron trajectory by bending the coaxial line. This varied the phase between the rf field in the sweep resonator and the entering electrons. It is easily seen that the resonator had to be shifted by only the length of a bunch (16 mm). The screen on which electron bunches were displayed contained a narrow horizontal slit, behind which an electron collector was placed to permit quantitative measurements. Electron density in the bunches was thus measured electrically besides being observed visually.

If the voltage in the accelerating resonator is  $U = U_0 \sin \omega t$ , the current in the last orbit traversing this resonator is some periodic function of phase or time  $J(\omega t)$ , which must be determined. The voltage in the sweep resonator was generally different in phase from that in the accelerating resonator, and would thus be described by

$\sin(\omega t + \varphi)$ .  $\varphi$  remains constant during the measurements. The current through the sweep resonator is\*

$$J(\omega t + \omega s/v) = J[\omega(t + s/v)], \quad (4)$$

where  $S$  is the length of the electron trajectory between the accelerating and the sweep resonator. The additional term  $\omega s/v$  depends on the electron time of flight from the former to the latter.

The only electrons passing through the slit in the screen will obviously be those traversing the sweep resonator close to the voltage phases  $2n\pi$ , i.e.,

$$\Omega t = 2n\pi - \varphi_1. \quad (5)$$

This phase region is given by

$$\Delta\varphi = \omega\tau, \quad (6)$$

where  $\tau$  is the time of beam passage through the slit;  $\tau = d/u$ , where  $d$  is the width of the slit,  $u = \omega A$  is the sweep speed, and  $A$  is the sweep (or deflection) amplitude (30–40 mm). In our case

$$\Delta\varphi = \omega d/u = d/A \approx 0.8^\circ. \quad (7)$$

During each period, for a given position of the sweep resonator the charge passing through the slit in the screen is

$$\left\{ J\left(\omega t + \omega \frac{s}{v}\right)_{\omega t = 2n\pi - \varphi_1} \right\} \tau = J\left(\omega \frac{s}{v} - \varphi_1\right) \frac{d}{\omega A}. \quad (8)$$

The mean current during a pulse is therefore

$$J\left(\omega \frac{s}{v} - \varphi_1\right) \frac{d}{\omega T A} = \frac{d}{2\pi A} J\left(\omega \frac{s}{v} - \varphi_1\right). \quad (9)$$

Multiplying by the duty cycle, we obtain the mean current at the collector:

$$J_c = \frac{d\nu_0\tau_0}{2\pi A} J\left(\omega \frac{s}{v} - \varphi_1\right), \quad (10)$$

where  $\nu_0$  is the pulse repetition rate and  $\tau_0$  is the pulse duration.

By varying the path  $s$  we obviously obtain  $J$ , the electron distribution, as a function of the phase. It is very clear that the measurements are essentially independent of the voltage amplitude in the sweep resonator, which determines only the resolution or accuracy of the method.

The sweep resonator (Fig. 2) was a toroidal resonant cavity with tapered capacitive bulges.

\*The current through the sweep resonator will generally be smaller than that through the accelerating resonator, because of the presence of a diaphragm. For the sake of simplicity we shall neglect this difference.

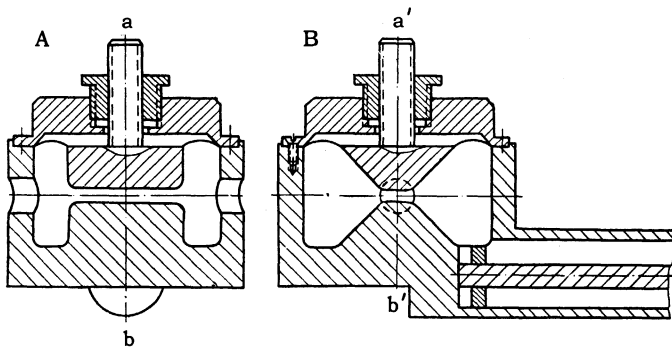


FIG. 2. Sweep resonator.

This resonator had to be positioned in the 12th orbit without encroaching on the 11th orbit; the distance between orbits was  $\sim \lambda/\pi = 32$  mm. This circumstance determined the shape of the resonator; a toroidal quasi-static resonator can be made considerably smaller than  $\lambda$ . The resonator was coupled inductively to the coaxial line by means of a bottom aperture (Fig. 2). A collar was moved along the center conductor of the line to regulate the coupling, which was adjusted to make the loaded  $Q$  of the resonator one-half of the unloaded value. There was thus no reflected wave in the coaxial line at resonance. The inner conductor had a 6-mm diameter, the inside diameter of the outer conductor was 14 mm, and the wave impedance of the line was  $\sim 50 \Omega$ .

The inner conductor was centered by means of teflon disks arranged to coincide with standing-wave voltage nodes in the resonator when untuned. The vacuum in the coaxial line was maintained through a number of openings in the outer conductor for the purpose of connecting the line to the microtron vacuum chamber. The line was connected to the waveguide (Fig. 1) by a stub terminating the center conductor. The coupling was varied within rather wide limits by changing the length of stub in the waveguide. The center conductor was a tube through which cooling water was circulated.

The shifting of the sweep resonator through bending of the coaxial line was performed by a selsyn-driven screw mechanism. For the purpose of investigating different parts of the electron beam, a cooled diaphragm with an aperture of 0.4-mm diameter, which could be shifted radially, was positioned in the last orbit ahead of the sweep resonator.

The fluorescent screen contained a horizontal slit 0.4 mm wide. The electron collector, a thick-walled lead Faraday cylinder, was located 110 mm behind the slit, and was connected to a high-sensitivity ( $10^{-12}$  amp) current amplifier. (The ampli-

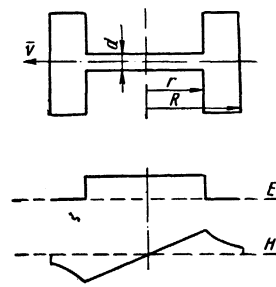


FIG. 3

fier of a standard "Cactus" dosimeter was used.) The high sensitivity of the amplifier required shielding of the Faraday cylinder from rf induction in the microtron chamber.

Signals from the amplifier were fed to an EPP-09 automatic potentiometer, whose tape motion was synchronized with the shifting of the sweep resonator. A curve representing the electron distribution in a bunch was thus traced automatically on the tape.

The production of a sufficiently large sweep amplitude on the screen required large rf power dissipation in the sweep resonator. For the purpose of calculating this power we considered the electron motion in the toroidal resonator (Fig. 3), where the field distribution was assumed to be quasi-stationary. The effect of the resonator magnetic field on the motion of a relativistic electron is of the same order of magnitude as that of the electric field and must be taken into account. Calculations showed that after traversing the sweep resonator an electron has the vertical momentum component

$$\Delta p_z = \frac{eE_0 \lambda}{c} \frac{\lambda}{2\pi} \cos(\varphi + \psi_0) \{ 2\sin\psi_1 - \psi_1^2 \text{Si}(\psi_0) - \text{Si}(\psi_1) \} - (\sin\psi_1 - \psi_1 \cos\psi_1), \quad (11)$$

where  $E_0$  and  $\lambda$  are the amplitude and wavelength of the electric field in the resonator,  $\varphi$  is the phase of electron transit through the center of the resonator,  $\psi_0 = 2\pi R/\lambda$ , and  $\psi_1 = 2\pi r/\lambda$ . The first term within the braces results from the electric field, while the second and third terms result from the magnetic field. These terms have the values 1.65,  $-0.38$ , and  $-0.27$ , respectively.

We thus see that the effect of the magnetic field is opposed to that of the electric field and equals 40% of the latter. The sweep amplitude  $A$  is related to the acquired momentum  $(\Delta p)_{\max}$  by

$$A = (\Delta p)_{\max} cL/E = (eE_0/E)L\lambda/2\pi, \quad (12)$$

where  $L$  is the distance from the resonator to the screen and  $E$  is the total electron energy. The electric field  $E_0$  is determined from the power absorbed in the resonator:

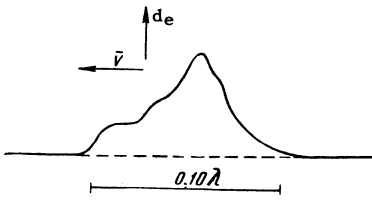


FIG. 4. Electron distribution along the length of a bunch.  $d_e$  is the electron density.

$$E_0 = \sqrt{8QW/fdr^2}, \quad (13)$$

where  $Q$  is the quality factor of the sweep resonator,  $W$  is the absorbed power,  $f$  is the frequency, and  $d$  and  $r$  are the resonator dimensions. The sweep amplitude is thus

$$A = (e/E)\sqrt{8QW/fdr^2}. \quad (14)$$

The parameters of our apparatus are  $Q = 3000$ ,  $L = 36$  cm,  $f = 3 \times 10^9$  cps,  $d = 0.8$  cm,  $r = 1.75$  cm.

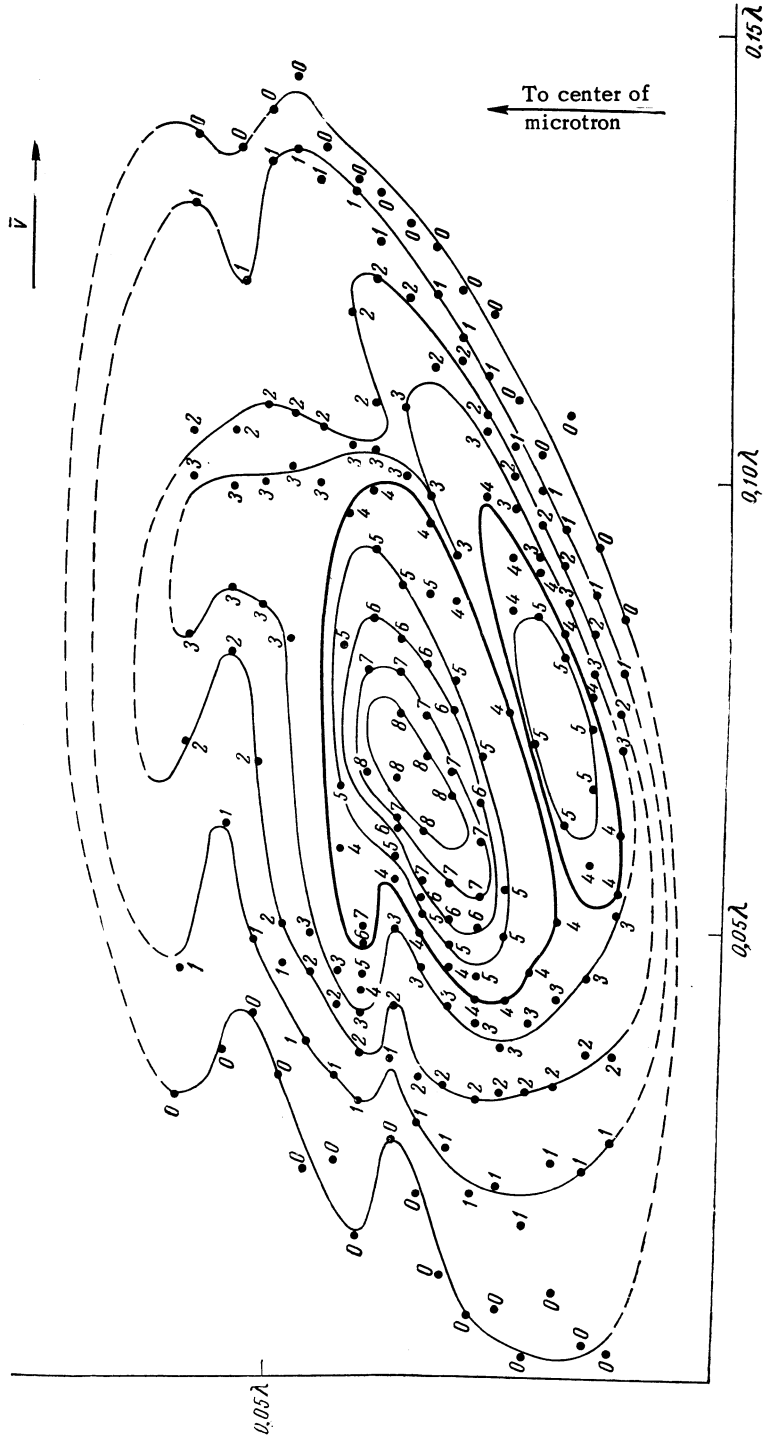


FIG. 5

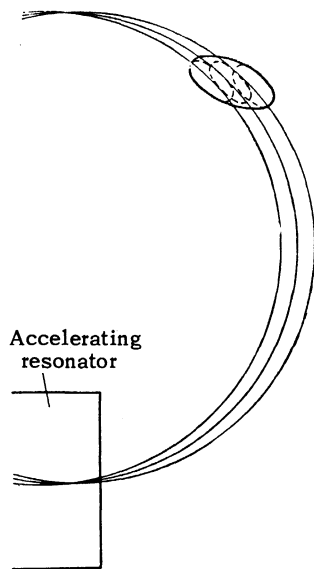


FIG. 6

and  $E = 7.3$  Mev. At the power level  $W = 40$  kw this gives the sweep amplitude  $A \approx 2.8$  cm. During the experiment the resonator absorbed 50–60 kw, and the sweep amplitude was 30–40 mm.

We shall now estimate the possible errors from several sources. First of all, when the coaxial line is bent the sweep resonator does not move along a circle but along a more complex curve, thus displacing the resonator with respect to the electron trajectory. Furthermore, since the beam is of finite width, it is shifted relative to the resonator axis. However, the field changes in the resonator close to the electron trajectory are proportional to the square of the displacement  $\Delta x$ :

$$\Delta E/E \sim \Delta H/H \sim (\Delta x/\lambda)^2. \quad (15)$$

We thus see that even with a 3-mm displacement the field change does not exceed some tenths of one percent and can be neglected.

Furthermore, the bending of the coaxial line changes its electrical length to some extent; this can change the phase in the sweep resonator. It is suggested by Krasnushkin's<sup>8</sup> investigation that the change of electrical length of the line as a fraction of the wavelength is

$$\Delta = l_0 a^2 / \lambda r^2, \quad (16)$$

where  $l_0$  is the length of the bent section,  $a$  is the radius of the line, and  $r$  is the radius of curvature of the bend. The actual radius of curvature was at least 200 cm. For  $a = 0.7$  cm and  $l_0 = 39$  cm we have  $\Delta = 5 \times 10^{-5}$ , corresponding to  $0.02^\circ$  phase difference, which is considerably below the resolving power of the apparatus. An experimen-

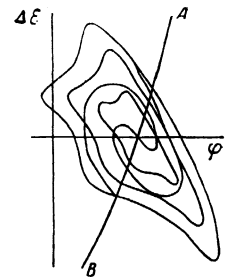


FIG. 7. Phase diagram.  $\Delta \epsilon$  is the departure of energy from equilibrium.

tal check showed that the phase change associated with the shifting of the resonator was under  $0.5^\circ$  in each instance.

Longitudinal displacement of the sweep resonator, changing the distance  $L$  to the screen, can also result in errors. The sweep speed will therefore differ for the measurements at the beginning and end of a bunch, respectively; the difference,  $\delta u/u = \delta L/L$ , is  $\sim 3\%$ . The electron density at the beginning of a bunch will therefore be about 3% greater than at the end. This error can be excluded by a suitable correction.

Finally, the electron energy spread ( $\pm 0.5\%$ )<sup>5,6</sup> also induces some error. The measurements will contain an error of the same magnitude, since the sweep speed is inversely proportional to the energy.

The pulsed operation of the microtron is also very important for the accuracy of the measurements. Oscillations are set up in the sweep resonator, with its smaller  $Q$ , more rapidly than in the accelerating resonator, where oscillations build up in  $1 \mu\text{sec}$ . However, the stable accelerating mode is established abruptly, since acceleration does not occur until the field amplitude in the accelerating resonator reaches a certain critical value.

An oscillogram of the accelerated current presents rectangular pulses  $2 \mu\text{sec}$  long with steep edges. The rise time does not exceed  $0.2 \mu\text{sec}$ . Thus the build-up processes cannot induce an error above 10%. The total systematic error of the measurements does not exceed 12–15%.

Figure 4 shows a typical record of the electron distribution in a bunch for a given diaphragm position. The electron density distribution over an entire bunch was determined by analyzing several plots corresponding to different diaphragm positions. The results are shown in Fig. 5, where the axes are parallel and perpendicular, respectively, to the direction of electron motion. The curves represent equal density levels bearing numbers proportional to the electron density.

The length of a bunch can be estimated from the diaphragm. If the length  $l$  is taken to mean the separation of two points where the electron density is half of the maximum, we have  $l \approx 0.05 - 0.07 \lambda$  or 5–7 mm.

The error in  $l$  resulting from cathode instability is 20–25%, based on repeated measurements. The operation of the microtron is stable for a few hours on the average. However, the stability requirements of our measurements were very rigorous; as a result, some instability of cathode emission appeared.

The existence of two maxima in a bunch has not previously been explained satisfactorily. The total length of a bunch is  $0.14\lambda$ , which considerably exceeds the theoretical length of the phase stability region ( $0.10\lambda$ ). This is accounted for by the angle spread in the velocities of electrons leaving the accelerating resonator. These electrons will therefore move along noncoincident orbits (Fig. 6), resulting in a lengthening of the bunches at orbital points most distant from the accelerating resonator.

In order to understand the electron distribution in a bunch we must consider how a phase diagram is filled in. Electrons emerging from the resonator for the first time are distributed uniformly along some curve AB intersecting the phase diagram (Fig. 7). In subsequent passes through the resonator this curve is transformed in a complex manner, since the frequency of phase oscillations depends on their amplitude. The curve ultimately just about fills the entire phase region. Some inhomogeneity of the magnetic field as well as possible fluctuations of the rf amplitude produces additional interspersions of electrons in the phase diagram. Electrons corresponding to large am-

plitudes of the phase oscillations will be smeared over a larger area than those close to the equilibrium position. This can obviously account for the experimentally observed electron distribution.

Incomplete coverage of the phase diagram by the shifting of the original curve would produce fine structure in a bunch. The second maximum in a bunch could possibly be the remnant of this fine structure.

I wish to thank P. L. Kapitza for his interest, and S. P. Kapitza for directing this research. I also wish to thank L. A. Vainshtein and V. N. Melekhin for many valuable discussions.

<sup>1</sup>V. I. Veksler, Doklady Akad. Nauk SSSR **43**, 346 (1944); J. Phys. U.S.S.R. **9**, 153 (1945).

<sup>2</sup>Redhead, Le Caine, and Henderson, Can. J. Phys. **A28**, 73 (1950).

<sup>3</sup>Henderson, Heymann, and Jennings, Proc. Phys. Soc. (London) **B66**, 654 (1953).

<sup>4</sup>S. P. Kapitza, Bykov, and Melekhin, JETP **39**, 997 (1960), Soviet Phys. JETP **12**, 693 (1961).

<sup>5</sup>Henderson, Heymann, and Jennings, Proc. Phys. Soc. (London) **B66**, 41 (1953).

<sup>6</sup>A. A. Kolomenskii, J. Tech. Phys. (U.S.S.R.) **30**, 1347 (1960), Soviet Phys.-Tech. Phys. **5**, 1278 (1961).

<sup>7</sup>L. É. Tzopp, Радиотехника и электроника (Radio Engineering and Electron Physics) **4**, 1936 (1959).

<sup>8</sup>P. E. Krasnushkin, Уч. зап. МГУ, (Science Notes, Moscow State University), Physics. v. **2**, No. 75, p. 9.